

## OPTICAL PROPERTIES OF ERBIUM DOPED ZnO FILMS GROWN ON DIFFERENT SUBSTRATES

V.F. GREMENOK

*State Scientific and Production Association "Scientific-Practical Materials Research Centre of the National Academy of Sciences of Belarus",  
220072, Minsk, P. Brovka Str. 19, Republic of Belarus*

The influence of post-deposition annealing at 600–900°C on optical properties of ZnO films co-doped with Erbium (Er) ions has been investigated by UV-V is, photoluminescence (PL) and photoluminescence excitation (PLE) methods. Er-doped ZnO (ZnO:Er) thin films were grown on fused quartz and *p*-Si substrates at 25°C by radio-frequency magnetron sputtering method. In accordance with the previously reported literature studies, post-growth annealing was required to activate the optical emission originated from the intra-shell transitions of the Er atoms. Transmission spectra of as-deposited Er-doped ZnO films contain a wide absorption band in the near-infrared region. It was found that an increase in the annealing temperature leads to an increase in the photoluminescence intensity in the spectral range of 1.5–3.0eV. PLE spectra of ZnO:Er films contain a band with a maximum at ~3.40eV which corresponds to the band gap energy of ZnO.

**Keywords:** ZnO:Er films, magnetron sputtering, optical properties, PL spectra.

**PACS:** 61.10.Kw, 68.37.-d, 78.20.-e, 78.30.Fs

### 1. INTRODUCTION

Rare-earth (RE) doped wide gap semiconductors have attracted considerable interest in recent years as a basis for optoelectronic devices, which combine the electronic properties of semiconductors with unique luminescence features of RE ions [1-8]. In recent years, the interest in preparing ZnO thin films doped with lanthanide elements (Ln<sup>3+</sup>) has increased due to the interesting properties that can be obtained by using 4f valence electron elements [2, 8]. It is well known that rare-earth ions (erbium, terbium, europium, thulium, and so on) are a special kind of photoactive centers with narrow emission lines and long emission lifetimes in various semiconductor materials. Erbium ion is one of the most popular lanthanides due to its radiative transitions in the green (0.56μm) and the infrared (1.54μm) being extensively used as an eye-safe source in the atmosphere, laser radar, medicine, and surgery [1,6,8]. Erbium acts as an optically active center if it is surrounded by oxygen forming a pseudo-octahedron structure. This means that Er replacing Zn in the ZnO matrix forms Er<sub>2</sub>O<sub>3</sub> and does not act as an optically active center. Therefore, an annealing treatment of thin films is required to change local structure of Er, forming clusters either in the ZnO matrix or at the grain boundaries.

Thin film growth parameters are largely affected by the deposition techniques and the process parameters. There are various deposition techniques available for preparing ZnO thin film [4, 9, 10]. One of the methods for ZnO film fabrication is radio-frequency (RF) magnetron sputtering. It results in the formation of columnar ZnO film with a preferred orientation of *c*-axes perpendicularly to the substrate surface. However, comparison of the results obtained for thin films, as far as we know, sometimes is contradictory. At the same time, the type of substrate can affect the structure as well as Er incorporation into ZnO films. Another important factor is the growth and annealing temperature for thin film formation.

This study is aimed at the synthesis and the optical

characterization of Er-doped ZnO thin films grown on fused quartz and *p*-Si substrates by radio-frequency magnetron sputtering with different dopant concentrations, as a function of post-growth annealing temperature at 600–900°C.

### 2. EXPERIMENTAL

ZnO:Er thin films were grown by RF magnetron sputtering of nominally pure Zn and ErCl<sub>3</sub>-targets in an argon atmosphere with oxygen (10% Ar and 90% O<sub>2</sub>) at a pressure of 5×10<sup>-3</sup> Torr on pure Si and fused quartz substrates at 25°C [11]. We used targets with erbium composition of 1% and 2% by mass. The power density applied to the cathode was 2.0W/cm<sup>2</sup> and the deposition time was 60 min. Both types of substrates were placed on the same sample holder to obtain the layers grown under the same conditions. The thickness of all films investigated was about 600–700nm. Isochronal (30–150min) post-growth annealing was performed at 600, 750, and 900°C in a conventional furnace in nitrogen flow. Chemical composition and the depth profile of elements in the films were determined by energy dispersive X-ray spectroscopy analysis (EDX) and Auger electron spectroscopy (AES) using a CAMECA SX-100 and Perkin Elmer Physics Electronic 590, respectively. The transmittance (T) spectra of the ErZO thin films onto quartz substrates were measured in the spectral range of 200–3000nm using a Carry 500 Scan UV-Vis-NIR (Varian, USA) spectrophotometer. Photoluminescence (PL) and photoluminescence excitation (PLE) measurements were carried out by employing a 1000 W Xe lamp as an excitation source combined with a grating monochromator (600 grooves/mm, focal length ~0.3m). All measurements were performed at room temperature.

### 3. RESULTS AND DISCUSSION

#### 3.1 Elemental composition of the films

The XRD spectra of the samples with different Er-compositions have peaks, which correspond of

hexagonal wurtzite ZnO [11]. The absence of Er-oxide related diffraction peaks indicates that there is no secondary phase in the films.

The composition of the thin films before and after the annealing was estimated from the EDX measurements and appeared to be invariable after the heat treatment. The chemical composition was determined by averaging the concentration values from

10 different points on the film surface (Table 1). The results show that the incorporation coefficient for  $Er^{+3}$  ions is approximately 1.5%. The EDX spectrum of Er-doped films shows the signals of Zn, O, Er, Si, C, and Ca where the signals of Si, C, Ca are from the substrates. Elemental mapping of Zn, Er, and O, shows a homogeneous distribution of all components without any concentrated places at the surface (not shown here).

Table 1  
Chemical composition of as-grown (i-ZnO) and ZnO:Er films fabricated on silicon and fused quartz substrates

| Sample    | Substrate | Annealing temperature, °C | Zn, at. % | O, at. % | Er, at. % |
|-----------|-----------|---------------------------|-----------|----------|-----------|
| i- ZnO    | Si        | 25                        | 49.9      | 50.1     |           |
| 1- ZnO:Er | Si        | 25                        | 48.7      | 50.5     | 0.8       |
| 2- ZnO:Er | Si        | 600                       | 49.1      | 50.1     | 0.8       |
| 3- ZnO:Er | Si        | 900                       | 49.3      | 50.0     | 0.7       |
| 4- ZnO:Er | quartz    | 25                        | 49.2      | 49.3     | 1.5       |
| 5- ZnO:Er | quartz    | 600                       | 49.5      | 49.1     | 1.4       |
| 6- ZnO:Er | quartz    | 900                       | 49.1      | 49.4     | 1.4       |

A similar elemental composition (Zn, O, Er in atomic %) of ZnO thin films has been confirmed by AES method. The spectra were analyzed over a range of kinetic energies from 100 to 1400eV using the primary electron beam of energy 5.0keV. The depth profile of elements for the as-grown and annealed samples on different substrates is shown homogeneous distribution of Zn, O, and Er along the depth of ZnO films. This fact confirmed the high-quality of the deposited films with nearly ideal stoichiometry of Zn and O chemical elements. The measurements show that

Er atomic concentration in ZnO is not exceeded 1.5 % at magnetron sputtering.

### 3.2 Optical and photoluminescence study

With the aim of the band gap energy determination of different ZnO:Er films fabricated on quartz substrates the measurements of reflectance spectra at room temperature have been performed. Figure 1 shows typical transmission spectra of the ZnO:Er thin films prepared on these substrates.

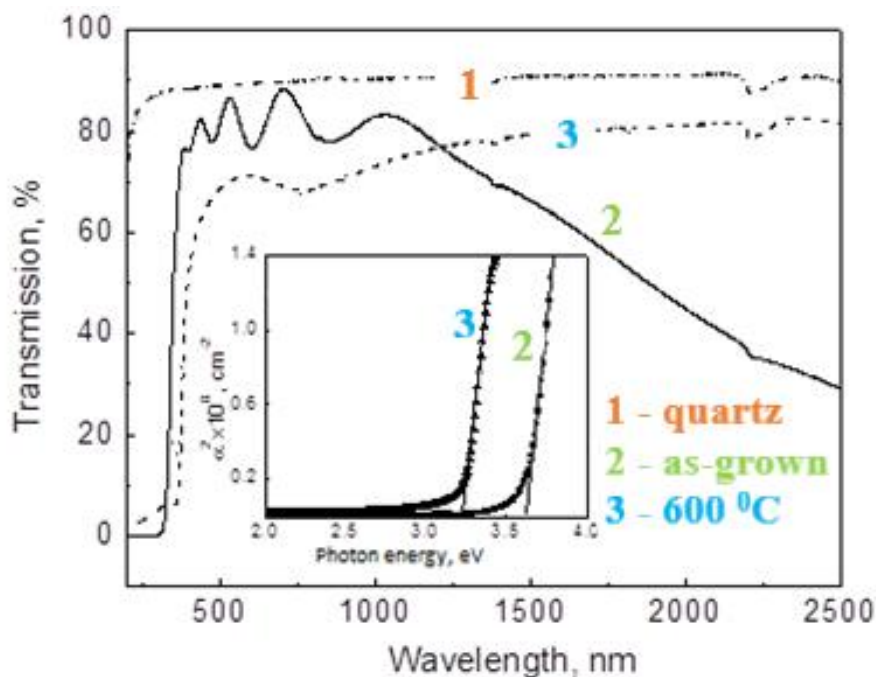


Fig. 1. Transmission spectra and the dependence of  $\alpha^2$  vs  $h\nu$  for ZnO:Er films on quartz substrates.

As seen all films have a high value of transmittance ~70 – 80% in wide spectral range 370-2500nm, intensive interference fringes, and a relatively sharp edge of the intrinsic absorption which starts at

less than 390nm. The sharp decrease in the transmission spectrum below ~450nm is related to the strong absorption of the photons in this region. These experimental data confirmed the high quality of

ZnO:Er material grown on quartz substrates. The shifting of intrinsic band edge in the ultraviolet spectral region and decreasing transmittance in the near-infrared region is observed for no annealed films in contrast to i-ZnO films. The absorption in  $1.0-2.5\mu\text{m}$  spectral region and high-energy shift of absorption edge are indicating strong doping effect of films by Er atoms. A similar behavior of optical spectra is observed for n-type highly doped semiconductors such as ZnO:Al [4, 12]. This phenomenon may be explained by the Burstein-Moss effect. The annealing at temperatures higher than  $600^\circ\text{C}$  leads to a low-energy shift of intrinsic absorption edge and decrease in infrared absorption.

The transmission spectra were analyzed under the light of Tauc expression and the derivative spectroscopy technique. The absorption coefficient ( $\alpha$ ) was calculated by the expression of  $\alpha = -\ln\tau/d$ , where the ZnO:Er film thickness is  $d \approx 700\text{nm}$ . Tauc formula is related with the band gap energy ( $E_g$ ) and the absorption coefficient [13]:

$$(\alpha h\nu) = A(h\nu - E_g)^n, \quad (1)$$

where  $A$  and  $n$  are band tailing parameters and index, respectively.

The  $n$  index is 2 for indirect and  $1/2$  for direct band gap energy characteristics. The Eq. (1) states that  $(\alpha h\nu)^{1/n}$  vs.  $(h\nu)$  plot exhibits a linear region in the strong absorption region. The linear fitted line intersects the energy axis at the band gap energy value. The  $(\alpha h\nu)^2$  vs.  $(h\nu)$  plots for ZnO:Er films are shown in the inset of Fig. 1. Amounts of  $E_g$  value are  $3.62\text{eV}$  and  $3.22\text{eV}$  for the as-deposited (4-ZnO:Er) and after annealing (5-ZnO:Er) films, respectively. These values are consistent with that measured from PLE spectra for the same samples.

The main attention was concentrated on the photoluminescence and photoluminescence excitation measurements of ZnO films prepared on different substrates. Figure 2 shows the photoluminescence and photoluminescence excitation spectra of i-ZnO thin films grown on  $p$ -type Si substrate after  $30\text{min}$  and subsequent annealing at temperatures of  $600^\circ\text{C}$ ,  $750^\circ\text{C}$  and  $900^\circ\text{C}$ .

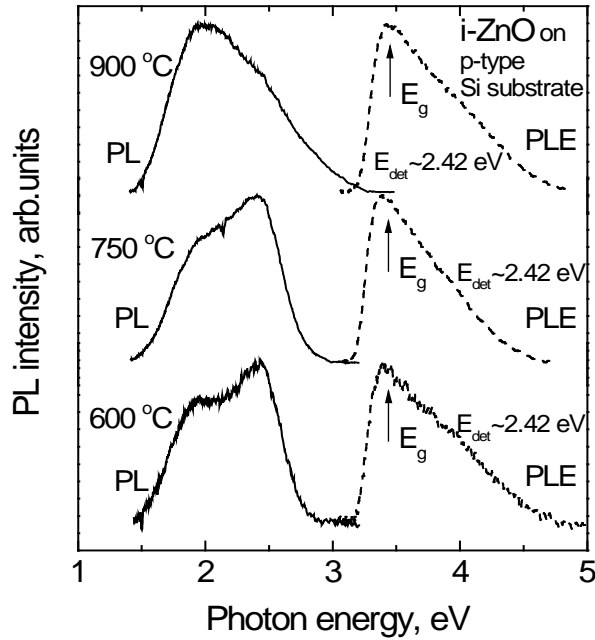


Fig. 2. PL and PLE spectra of i-ZnO thin films for different annealing temperature.

The PL and PLE spectra were taken at room temperature. It is clearly seen that PL spectra contain two broad intense bands with maxima at  $2.43\text{eV}$  (green emission  $510\text{nm}$ ) and at  $1.94\text{eV}$  (yellow emission at  $640\text{nm}$ ). The experiments show that the relative intensity of green and yellow emissions increases with annealing temperature reaching a maximum at  $900^\circ\text{C}$ . The annealing time in the range from 30 up to 150 min for each temperature also increases the intensity of the bands at  $2.43\text{eV}$  and  $1.94\text{eV}$ . These two bands may be referred to oxygen vacancy ( $V_{\text{O}}^+$ ) and oxygen interstitial ( $\text{O}_i^-$ ) respectively. The changes in the relative intensity of both bands are observed at annealing temperature variation. This effect indicates redistribution of radiative recombination channels of nonequilibrium charge carriers. Figure 2 shows that the

green-dominant emission at lower annealing temperature ( $600^\circ\text{C}$  and  $750^\circ\text{C}$ ) is switched to yellow emission at higher annealing temperature ( $900^\circ\text{C}$ ). This is issued by the competition between the formation of  $V_{\text{O}}^+$  and  $\text{O}_i^-$  defects. A broad PLE band with a maximum at  $3.40\text{eV}$  was observed for all investigated i-ZnO films. The energy maximum at  $3.40\text{eV} \pm 0.05\text{eV}$  corresponds to the optical band gap energy of ZnO material [4].

Figure 3 shows the PL and PLE spectra for Er-doped ZnO thin films on Si substrate. The deposited films were annealed at different temperatures. When the annealing temperature increased in the range  $600-900^\circ\text{C}$  high strength deep-level emission in the spectral region  $1.5-3.0\text{eV}$  has been observed.

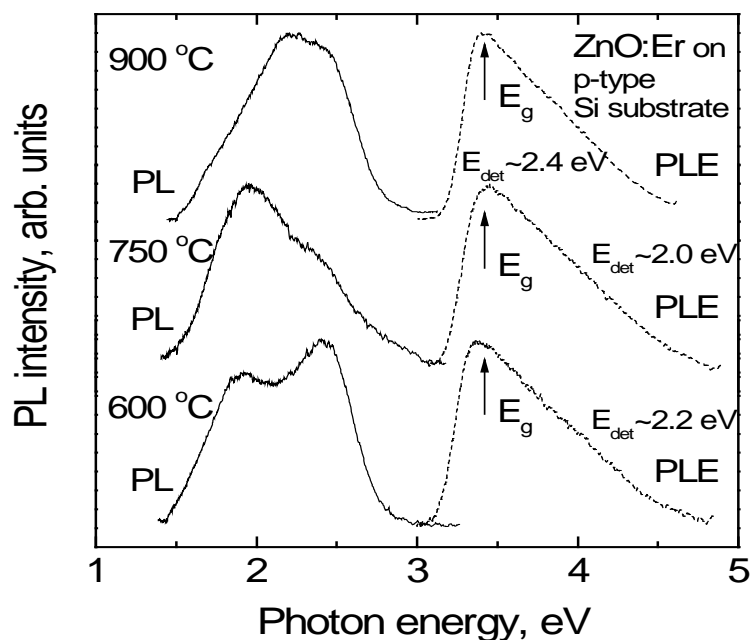


Fig. 3. PL and PLE spectra of ZnO:Er thin films for different annealing temperature.

It can be seen that the peak intensity and energy position of deep-level emission varies with annealing temperatures. In particular, ZnO:Er films annealed at 900 °C show only one broad PL band. The appearance of this band may be related to the formation of defects induced by Er atom incorporation in the ZnO lattice. The rate of formation point defects is low for ZnO:Er films annealed at low temperature  $\sim 600^\circ\text{C}$ . More defects responsible for the radiative transitions introduce into the films for the temperatures higher than 600 °C. In addition to thermal treatment, doping by Er atoms play an important role in the mechanism responsible for the deep-level luminescence as well. It is notable that the yellow emission decreases with increasing annealing temperature for Er-doped ZnO thin films. One cause is most likely due to the formation of Er- $V_{\text{O}}$  bonds in ZnO:Er films. Another possibility of the variation in the intensity of the yellow band at  $\sim 1.94\text{eV}$  can be ascribed to the additional formation of interstitial oxygen. The probability of the electron charge transfer from localized impurity states to the conductive states is increased due to the potential fluctuation of Er impurities in ZnO films. We must speculate that both probable mechanisms are responsible for the increase of green emission. Further investigations are needed to verify this point of view. The PLE spectra of films also contain broad band with a maximum at  $3.40 \pm 0.05\text{eV}$  which corresponds to the optical band gap energy of ZnO.

It is well known that  $\text{Er}^{3+}$  ions are responsible for the visible luminescence in the spectral region 500–600 nm (2.07–2.48 eV) [2, 6, 14]. We cannot have detected sharp  $\text{Er}^{3+}$  related lines in the green region of spectra due to high-intensity emission related to intrinsic point defects such as  $\text{O}_i$  and  $\text{V}_\text{O}$  in ZnO material. Instead that we detected infrared

luminescence of  $\text{Er}^{3+}$  in films (Fig. 4, 5). It is clearly seen that ZnO:Er films exhibited  $1.54(0.81\text{eV})\mu\text{m}$   $\text{Er}^{3+}$  photoluminescence [15, 16]. This fact strongly suggests that  $\text{Er}^{3+}$  ions were incorporated in the ZnO lattice during the magnetron sputtering process. The Er emission mechanism under indirect excitation is generally explained using an energy transfer model [2, 8]. In the thin film and or bulk counterparts of Er doped ZnO, the necessity of annealing to obtain the  $1.54\mu\text{m}$  luminescence is explained by Er site activation. It has been found that the higher order O coordination around the Er decreased the PL intensity, which could be significantly improved when the local structure of the Er-O cluster changed to a pseudo-octahedron with  $\text{C}_{4v}$  symmetry [17].

The PLE spectra of the infrared luminescence of Er-doped ZnO films on different substrates as a function of excitation wavelength showed that infrared  $\text{Er}^{3+}$  related emission may be excited by the band-to-band mechanisms in ZnO material as well as upper above gap excitation (Fig. 4, 5). The relatively intense broad band at  $3.2\text{eV}$  was detected in the PLE spectra for the different stages of the annealing.

A more interesting experimental finding is the efficient excitation of  $\text{Er}^{3+}$ -related emission near  $1.54\mu\text{m}$  (0.81 eV) throughout the band at  $3.2\text{eV}$  in comparing with band-to-band optical transition in PLE spectra of ZnO:Er thin films. The band at  $3.2\text{eV}$  in PLE spectra (Fig. 4, 5) may be attributed to the transitions on Er - O defects with relatively shallow energy levels in thin films [2, 6, 14]. An increase in the intensity of the PLE band at  $3.2\text{eV}$  with increasing annealing temperature results from the increasing concentration of structural Er-O defects and the formation of impurity energy band with shallow levels [6 - 8].

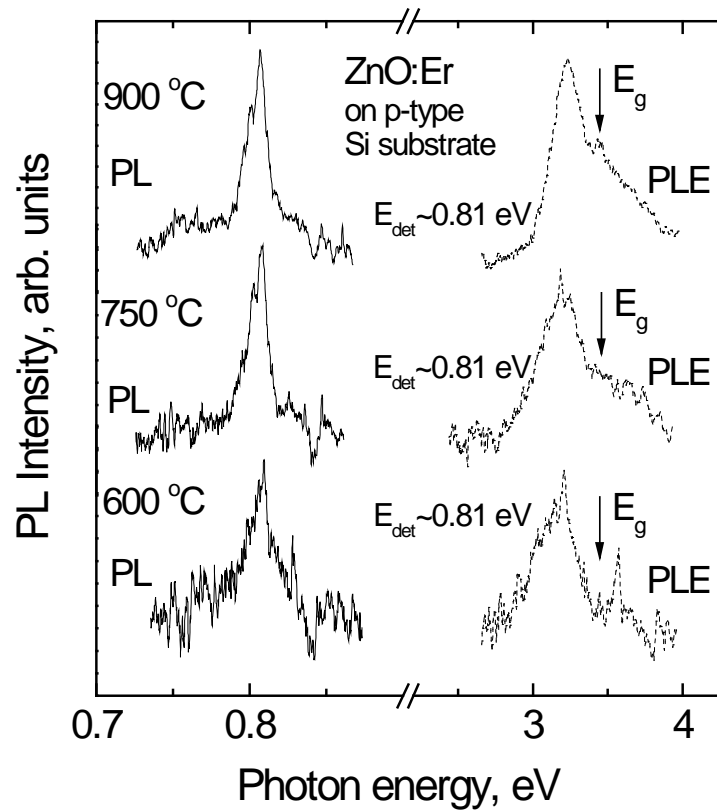


Fig. 4. PL and PLE spectra of ZnO:Er thin films on Si substrates for different annealing temperature.

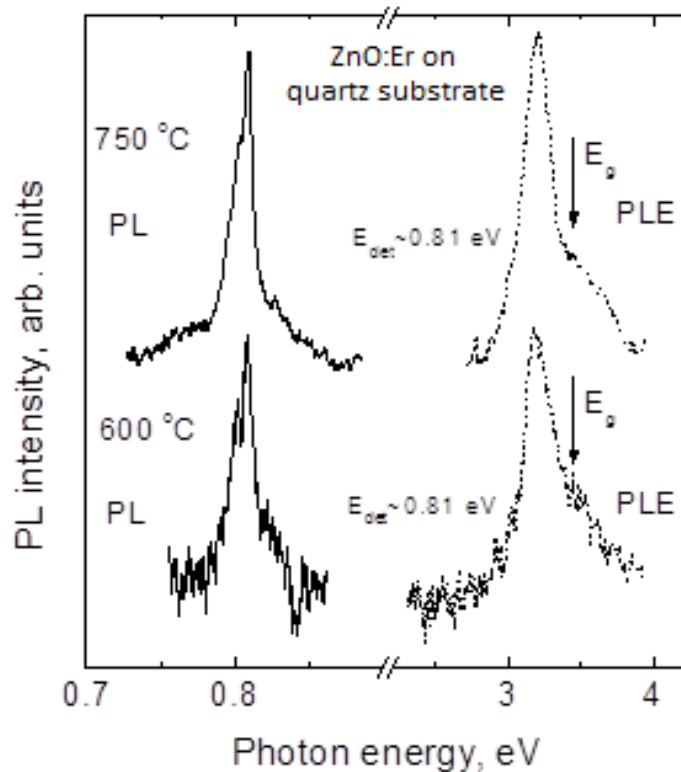


Fig. 5. PL and PLE spectra of ZnO:Er thin films on quartz substrate for different annealing temperature.

#### 4. CONCLUSIONS

The effect of different atomic contents of  $\text{Er}^{+3}$  ions on optical and photoluminescence properties of ZnO films grown on fused quartz and  $p$ -Si substrates was

studied by different experimental techniques. All investigated films were found by XRD to have a polycrystalline wurtzite type structure. The doped ZnO films showed good transmittances (70–80%) in the spectral range of 370–2500nm. The annealing at

temperatures higher than  $600^{\circ}\text{C}$  in nitrogen flow of these films leads to a low-energy shift of intrinsic absorption edge. After post-annealing treatment of ZnO:Er films green and near  $1.54\mu\text{m}$  PL emission related to intra- $4f$  shell of  $\text{Er}^{3+}$  ions are observed. The relatively intense broad band at  $3.2\text{eV}$  has been found in the PLE spectra for the different stages of the annealing and may be attributed to the optical transitions on Er-O defects with relatively shallow energy levels in ZnO:Er material. The PLE spectra of ZnO:Er thin films on different substrates also contain broad band with a maximum of  $3.40 \pm 0.05\text{eV}$  which corresponds to the band gap energy of pure ZnO. Our results indicate that  $\text{Er}^{3+}$  ions are an effective co-doping

element for ZnO films that can be used for application in thin film solar cells, laser and display technologies.

## 5. ACKNOWLEDGMENTS

The work has been financed by the Belarusian State Programme for Research «Physical Material Science, New Materials and Technologies». The author of this work is grateful to Affiliate RDC “Belmicrosystems” JSC “INTEGRAL”-“INTEGRAL” Holding Managing Company for EDX study of thin films.

- 
- [1] S. Hufner. Optical Spectra of Transparent Rare Earths Compounds. Academic Press, New York, San Francisco, London, 1978, p.237.
- [2] A.J. Kenyon. Prog. Quantum Electron. 2002, vol.26, pp.225–284.
- [3] P.C. de Sousa Filho, J.F. Lima, O.A. Serra, J. Braz. Chem. Soc., 2015, vol.26 (12), pp.2471-2495.
- [4] V.A. Coleman, A. Victoria, C. Jagadish. Basic Properties and Applications of ZnO, Zinc Oxide Bulk, Thin Films and Nanostructures. Elsevier Science Ltd, Amsterdam, 2006, p.589.
- [5] Y.S. Park, C.W. Litton, T.C. Collins, D.C. Reynolds. Phys. Rev., 1966, vol.143, pp.512–519.
- [6] A. Polman. Journal of Applied Physics, 1997, vol.82, pp.1–39.
- [7] H. Akazawa, H. Shinjima. Mater. Sci. Eng. B., 2014, vol.189, pp.38–44.
- [8] V. Kumar, O.M. Ntwaeaborwa, T. Soga, V. Dutta, H.C. Swart. ACS Photonics, 2017, vol.4, pp.2613–2637.
- [9] Y.K. Mishra, G. Modi, V. Cretu, V. Postica, O. Lupan, T. Reimer, I. Paulowicz, R. Adelung. ACS Appl. Mater. Interfaces, 2015, vol.7, pp.14303–14316.
- [10] Z.L. Wang. Journal of Physics: Condensed Matter, 2004, vol.16, pp.R829–R858.
- [11] V. Malyutina-Bronskaya, A. Semchenko, V. Sidsky, V. Fedorov, V. Saladukha, A. Perets. Proceedings of the IEEE 7th International Conference on Nanomaterials: Applications and Properties, 2017, pp.02NTF23-1-02NTF23-3.
- [12] N.H. Nickel, E. Terukov. Zinc Oxide - A Material for Micro - and Optoelectronic Applications, Springer, Netherlands, 2005, p.240.
- [13] J.I. Pankove. Optical Processes in Semiconductors, Prentice-Hall, Englewood Cliffs, New Jersey, 1971, p.422.
- [14] A.J. Kenyon. Prog. Quantum Electron, 2002, vol.26, pp.225–284.
- [15] T. Schmidt, G. Muller, L. Spanhel, K. Kerkel, A. Forchel. Chem. Mater., 1998, vol.10, pp.65–71.
- [16] Juan Wang, M.J. Zhou, S.K. Hark, D. Tang, M.W. Chu, C.H. Chen. Appl. Phys. Lett., 2006, vol.89, pp.221917.
- [17] M. Ishii, S. Komuro, T. Morikawa, Y. Aoyagi. J. Appl. Phys., 2001, vol.89, pp.3679-3684.

Received: 02.02.2022